Contribution 19

Impact of semi-annihilations on dark matter phenomenology – an example of Z_N symmetric scalar dark matter

G. Bélanger, K. Kannike, A. Pukhov, M. Raidal

Abstract

We study the impact of semi-annihilations $\chi\chi \leftrightarrow \chi X$, where χ is dark matter and X is any standard model particle, on dark matter phenomenology. We formulate scalar dark matter models with minimal field content that predict non-trivial dark matter phenomenology for different discrete Abelian symmetries Z_N, $N > 2$, and contain semi-annihilation processes. We implement such an example model in micrOMEGAs and show that semi-annihilations modify the phenomenology of this type of models.

1 INTRODUCTION

The origin of dark matter of the Universe is not known. In popular models with new particles beyond the standard model particle content, such as the minimal supersymmetric standard model, an additional discrete Z_2 symmetry is introduced [514]. As a result, the lightest new Z_2-odd particle, χ, is stable and is a good candidate for dark matter. The phenomenology of this type of models is studied extensively.

The discrete symmetry that stabilises dark matter must be the discrete remnant of a broken gauge group [515], because global discrete symmetries are broken by gravity. The most natural way for the discrete symmetry to arise is from breaking of a $U(1)_X$ embedded in a larger gauge group, e.g. $SO(10)$ [516]. The latter contains gauged $B - L$ as a part of the symmetry, and the existence of dark matter can be related to the neutrino masses, leptogenesis and, in a broader context, to the existence of leptonic and baryonic matter [299, 303, 517].

Obviously, the discrete remnant of $U(1)_X$ need not to be Z_2 – in general it can be any Z_N Abelian symmetry. The possibility that dark matter may exist due to Z_N, $N > 2$, is a known [354,518–525] but much less studied scenario[1]. Model independently, it has been pointed out in Ref. [525] that in Z_N models the dark matter annihilation processes contain new topologies with different number of dark matter particles in the initial and final states – called semi-annihilations –, for example $\chi\chi \leftrightarrow \chi X$, where X can be any standard model particle. It has been argued that those processes may significantly change the predictions for generation of dark matter relic abundance in thermal freeze-out. However, no detailed studies have been performed that compare dark matter phenomenology of different Z_N models. This is difficult also because presently the publicly available tools for computing dark matter relic abundance do not include the possibility of imposing Z_N discrete symmetry instead of Z_2.

[1] Phenomenology of Z_3-symmetric dark matter in supersymmetric models has been studied in Refs. [518, 520] and in extra dimensional models in Refs. [354, 519].

The aim of this work is to formulate the minimal scalar dark matter model that predicts different non-trivial scalar potentials for different Z_N symmetries and to study their phenomenology. In particular we are interested in quantifying the possible effects of semi-annihilation processes $\chi\chi \leftrightarrow \chi X$ on generating the dark matter relic abundance. In order to perform quantitatively precise analyses we implement minimal Z_3 symmetric scalar dark matter models that contain one singlet and one extra doublet in micrOMEGAs [206, 526]. Using this tool we show that, indeed, the semi-annihilations affect the dark matter phenomenology and should be taken into account in a quantitatively precise way in studies of any particular model.

2 Z_N LAGRANGIANS

2.1 Z_N symmetry

Under an Abelian Z_N symmetry, where N is a positive integer, addition of charges is modulo N. Thus the possible values of Z_N charges can be taken to be $0, 1, \ldots, N-1$ without loss of generality. A field ϕ with Z_N charge X transforms under a Z_N transformation as $\phi \to \omega^X \phi$, where $\omega^N = 1$, that is $\omega = \exp(i2\pi/N)$.

A Z_N symmetry can arise as a discrete gauge symmetry from breaking a $U(1)_X$ gauge group with a scalar whose X-charge is N [515, 517].

For larger values of N the conditions the Z_N symmetry imposes on the Lagrangian approximates a $U(1)$ symmetry for two reasons. First, assuming renormalizability, the number of possible Lagrangian terms is limited and will be exhausted for some small finite N, though they may come up in different combinations for different values of N. Second, if the Z_N symmetry arises from some $U(1)_X$, the X-charges of particles cannot be arbitrarily large, because that would make the model nonperturbative – if N is larger than the largest charge in the model, the restrictions on the Lagrangian are the same as in the unbroken $U(1)$.

We shall see below that for the large number of possible assignments of Z_N charges to the fields, the number of possible distinct potentials is much smaller.

2.2 Field content of the minimal model

In order to study how different discrete Z_N symmetries impact dark matter phenomenology the example model must contain more than one type of dark matter candidates. The minimal dark matter model that possesses such properties contains, in addition to the standard model fermions and the standard model Higgs boson H_1, one extra scalar doublet H_2 and one extra complex scalar singlet S [299]. In the case of Z_2 symmetry, as proposed in [299], those new fields can be identified with the well known inert doublet H_2 [527–530] and the complex singlet S [295–298, 302]. The phenomenology of those models is well studied. However, when they are put together, qualitatively new features concerning dark matter phenomenology, electroweak symmetry breaking and collider phenomenology occur [299, 303, 531–533]. The field content of the minimal scalar Z_N model is summarized in Table 1.

Table 1: Scalar field content of the low energy theory with the components of the standard model Higgs H_1 in the Feynman gauge. The value of the Higgs VEV is $v = 246$ GeV.

Field	$SU(3)$	$SU(2)_L$	T^3	$Y/2$	$Q = T^3 + Y/2$
$H_1 = \begin{pmatrix} G^+ \\ \frac{v+h+iG^0}{\sqrt{2}} \end{pmatrix}$	$\mathbf{1}$	$\mathbf{2}$	$\begin{pmatrix} \frac{1}{2} \\ -\frac{1}{2} \end{pmatrix}$	$\frac{1}{2}$	$\begin{pmatrix} 1 \\ 0 \end{pmatrix}$
$H_2 = \begin{pmatrix} H^+ \\ \frac{H^0+iA^0}{\sqrt{2}} \end{pmatrix}$	$\mathbf{1}$	$\mathbf{2}$	$\begin{pmatrix} \frac{1}{2} \\ -\frac{1}{2} \end{pmatrix}$	$\frac{1}{2}$	$\begin{pmatrix} 1 \\ 0 \end{pmatrix}$
$S = \frac{S_H+iS_A}{\sqrt{2}}$	$\mathbf{1}$	$\mathbf{1}$	0	0	0

2.3 Constraints on charge assignments

The assignments of Z_N charges have to satisfy

$$\begin{aligned} X_S &> 0, \\ X_1 &\neq X_2, \\ -X_\ell + X_1 + X_e &= 0 \mod N, \\ -X_q + X_1 + X_d &= 0 \mod N, \\ -X_q - X_1 + X_u &= 0 \mod N. \end{aligned} \tag{1}$$

The first and second conditions arise from avoiding the $|H_1|^2 S$ term and from avoiding Yukawa terms for H_2, respectively, and the rest from requiring Yukawa terms for H_1.

The choice of Z_N charges for standard model fermions, the standard model Higgs H_1, the inert doublet H_2 and the complex singlet S must be such that there are no Yukawa terms for H_2 and no mixing between H_1 and H_2: only annihilation and semiannihilation terms for H_2 and S are allowed.

All possible scalar potentials contain a common piece because the terms where each field is in pair with its Hermitian conjugate are allowed under any Z_N and charge assignment. We denote it by V_c, where the 'c' stands for 'common':

$$\begin{aligned} V_\mathrm{c} = {} & \mu_1^2|H_1|^2 + \lambda_1|H_1|^4 + \mu_2^2|H_2|^2 + \lambda_2|H_2|^4 + \mu_S^2|S|^2 + \lambda_S|S|^4 \\ & + \lambda_{S1}|S|^2|H_1|^2 + \lambda_{S2}|S|^2|H_2|^2 + \lambda_3|H_1|^2|H_2|^2 + \lambda_4(H_1^\dagger H_2)(H_2^\dagger H_1). \end{aligned} \tag{2}$$

2.4 The Z_2 scalar potential

There are 256 ways to assign $0, 1$ to the standard model and dark sector fields. Of these, 8 satisfy Eq. (1); among them, there are 2 different assignments to the dark sector fields, both

giving rise to the unique scalar potential

$$
\begin{aligned}
V = V_{\rm c} &+ \frac{\mu_S'^2}{2}(S^2 + S^{\dagger 2}) + \frac{\lambda_5}{2}\left[(H_1^\dagger H_2)^2 + (H_2^\dagger H_1)^2\right] \\
&+ \frac{\mu_{SH}}{2}(S^\dagger H_1^\dagger H_2 + S H_2^\dagger H_1) + \frac{\mu'_{SH}}{2}(S H_1^\dagger H_2 + S^\dagger H_2^\dagger H_1) \\
&+ \frac{\lambda'_S}{2}(S^4 + S^{\dagger 4}) + \frac{\lambda''_S}{2}|S|^2(S^2 + S^{\dagger 2}) \\
&+ \lambda_{S1}|S|^2|H_1|^2 + \lambda_{S2}|S|^2|H_2|^2 \\
&+ \frac{\lambda'_{S1}}{2}|H_1|^2(S^2 + S^{\dagger 2}) + \frac{\lambda'_{S2}}{2}|H_2|^2(S^2 + S^{\dagger 2}).
\end{aligned}
\tag{3}
$$

2.5 Z_3 scalar potentials

There are 6561 ways to assign $0, 1, 2$ to the fields. Of these, 108 satisfy Eq. (1); among them, there are 12 different assignments to the dark sector fields, giving rise to 2 different scalar potentials. The example potential we choose to work with is

$$
\begin{aligned}
V_{Z_3} = V_{\rm c} &+ \frac{\mu''_S}{2}(S^3 + S^{\dagger 3}) + \frac{\lambda_{S12}}{2}(S^2 H_1^\dagger H_2 + S^{\dagger 2} H_2^\dagger H_1) \\
&+ \frac{\mu_{SH}}{2}(S H_2^\dagger H_1 + S^\dagger H_1^\dagger H_2),
\end{aligned}
\tag{4}
$$

which induces the semi-annihilation processes we are interested in. The second one is obtained from Eq. (4) by changing $S \to S^\dagger$ (with $\mu_{SH} \to \mu'_{SH}$ and $\lambda_{S12} \to \lambda_{S21}$).

2.6 Z_4 scalar potentials

There are 65536 ways to assign $0, 1, 2, 3$ to the fields. Of these, 576 satisfy Eq. (1); among them, there are 36 different assignments to the dark sector fields, giving rise to 5 different scalar potentials. Among those the only potential that contains semi-annihilation terms is

$$
\begin{aligned}
V^1_{Z_4} = V_{\rm c} &+ \frac{\lambda'_S}{2}(S^4 + S^{\dagger 4}) + \frac{\lambda_5}{2}\left[(H_1^\dagger H_2)^2 + (H_2^\dagger H_1)^2\right] \\
&+ \frac{\lambda_{S12}}{2}(S^2 H_1^\dagger H_2 + S^{\dagger 2} H_2^\dagger H_1) + \frac{\lambda_{S21}}{2}(S^2 H_2^\dagger H_1 + S^{\dagger 2} H_1^\dagger H_2).
\end{aligned}
\tag{5}
$$

The other four scalar potentials can be formally obtained from the Z_2-invariant potential Eq. (3) by setting all the new terms added to $V_{\rm c}$ to zero, with the exception of the 1) λ'_S, μ_{SH}, 2) λ'_S, μ'_{SH}, 3) μ'_S, λ'_S, λ''_S, λ'_{S1}, λ'_{S2}, 4) μ'_S, λ'_S, λ''_S, λ'_{S1}, λ'_{S2}, μ_{SH}, μ'_{SH} terms.

3 RELIC DENSITY IN CASE OF THE Z_3 SYMMETRY

3.1 Evolution equations

Consider the Z_3-symmetric theory. The imposed Z_3 symmetry implies, as usual, just one dark matter candidate. This is because the Z_3 charges 1 and -1 correspond to particle and anti-particle. The new feature is that processes of the type $\chi\chi \to \chi X$, where X is any standard model particle, also contribute to dark matter annihilation. The equation for the number density reads

$$
\frac{dn}{dt} = -v\sigma_{\chi\chi\to XX}\left(n^2 - n_{\rm eq}^2\right) - \frac{1}{2}v\sigma_{\chi\chi\to\chi X}\left(n^2 - n\, n_{\rm eq}\right) - 3Hn. \tag{6}
$$

We define

$$\sigma_v = v\sigma_{\chi\chi\to XX} + \frac{1}{2}v\sigma_{\chi\chi\to\chi X}v \quad \text{and} \quad \alpha = \frac{1/2\sigma_{\chi\chi\to\chi X}}{\sigma_v}, \tag{7}$$

which means that $0 \leq \alpha \leq 1$. In terms of the abundance, $Y = n/s$, where s is the entropy density, we obtain

$$\frac{dY}{dt} = -s\sigma_v \left(Y^2 - \alpha Y Y_{\rm eq} - (1-\alpha)Y_{\rm eq}^2\right) \tag{8}$$

or

$$\frac{dY}{ds} = \frac{\sigma_v}{H}\left(Y^2 - \alpha Y Y_{\rm eq} - (1-\alpha)Y_{\rm eq}^2\right). \tag{9}$$

To solve this equation we follow the usual procedure [526]. Writing $Y = Y_{\rm eq} + \Delta Y$ we find the starting point for the numerical solution of this equation using the Runge-Kutta method using

$$\frac{dY_{\rm eq}}{ds} = \frac{\sigma_v}{H}Y\Delta Y\,(2-\alpha)\,, \tag{10}$$

where $\Delta Y \ll Y$. This is similar to the standard case except that ΔY increases by a factor $1/(1-\alpha/2)$. Furthermore, when solving numerically the evolution equation, the decoupling condition $Y^2 \gg Y_{\rm eq}^2$ is modified to

$$Y^2 \gg \alpha Y Y_{\rm eq} + (1-\alpha)Y_{\rm eq}^2. \tag{11}$$

This implies that freeze-out starts at an earlier time and lasts until a later time as compared with the standard case. This modified evolution equation is implemented in micrOMEGAs [206, 208].

3.2 Numerical results with micrOMEGAs

Using the scalar potential defined in Eq. (4) we have implemented in micrOMEGAs the scalar model with a Z_3 symmetry. The scalar sector is composed of one additional complex scalar doublet and one complex singlet. The neutral component of the doublet mixes with the singlet, the lightest component $\tilde{h}_1$ is therefore the dark matter candidate, while the heavy component $\tilde{h}_2$ can decay into $\tilde{h}_1 h$, where h is the standard model like Higgs boson. The Z_3 charge of $\tilde{h}_1, \tilde{h}_2, \tilde{h}^+$ is 1.

We then compute the dark matter relic density as well as the elastic scattering cross section on nuclei. Here we average over dark matter and anti-dark matter cross section assuming that they have the same density. the main contribution here comes from the Z-exchange diagram because there is a $\tilde{h}_1\tilde{h}_1^* Z$ coupling[2]. Furthermore one can easily show that the scattering amplitudes are not the same for protons and neutrons. Since the current experimental bounds on $\sigma_{\chi n}^{\rm SI}$ are extracted from experimental results assuming that the couplings to protons (f_p) and neutrons (f_n) are equal, we define the normalized cross section on a point-like nucleus [237]:

$$\sigma_{\tilde{h}_1 N}^{\rm SI} = \frac{\mu_{\psi_1}^2}{\pi}\frac{[Zf_p + (A-Z)f_n]^2}{A^2}\,. \tag{12}$$

This quantity can directly be compared with the limit on $\sigma_{\chi n}^{\rm SI}$.

[2]In the inert doublet model with a Z_2 symmetry [527, 529], a λ_5 term splits the complex doublet into a scalar and a pseudoscalar, when the mass splitting is small such coupling leads to inelastic scattering.

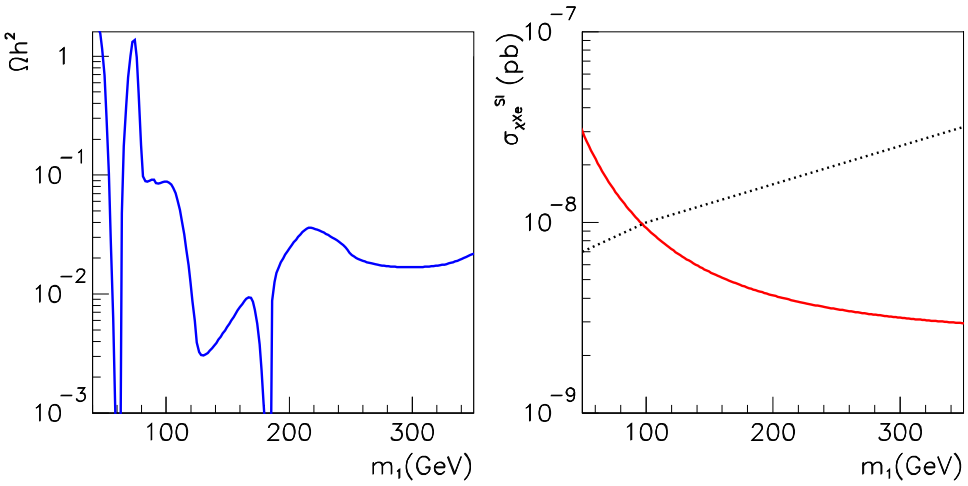

Figure 1: Ωh^2 as a function of the dark matter mass (left panel) and $\sigma^{\rm SI}_{\tilde{h}_1 Xe}$. The experimental limit from XENON100 [196] is also displayed (dashed line.)

To illustrate the behavior of the relic density of dark matter, we choose the parameters $\lambda_2 = 0.73, \lambda_3 = 0.16, \lambda_4 = 0.45, \lambda_S = 0.93$, $\lambda_{S1} = 0.06$, $\lambda_{S2} = 0.03, \lambda_{S21} = 0.69$, $\mu''_S = 427.5$ GeV. Furthermore we fix the mass of the Higgs sector to be $M_h = 125$ GeV, $M_{h_2} = 371.2$ GeV and let $M_{\tilde{h}_1}$ vary. We also assume that $\tilde{h}_1$ is almost singlet taking $\sin\theta_h = 0.9995$.

The variation of Ωh^2 with the dark matter mass is displayed in Fig. 1. When the dark matter mass is around 50 GeV the main annihilation channel is through Z-exchange, note that this, however, leads to a very large direct detection rate. As $m_1 = m_{\tilde{h}_1}$ increases above $m_Z/2$, the relic density increases dramatically. At this point α is very small since the process $\tilde{h}_1\tilde{h}_1 \to \tilde{h}_1^* Z$ is kinematically forbidden. After the threshold for W pair production, the relic density starts to drop, the process $\tilde{h}_1\tilde{h}_1 \to \tilde{h}_1^* Z$ soon becomes kinematically accessible and α increases rapidly. The contribution of this channel rises rapidly leading to a drop of Ωh^2 to values below the preferred region extracted form WMAP measurements [284]. For yet larger dark matter masses the annihilation process $\tilde{h}_1\tilde{h}_1 \to h_2^* \to \tilde{h}_1^* h$ occurs near the h_2 resonance, this is the second drop in Ωh^2 displayed in Fig. 1. As the dark matter mass increases further, several processes involving one non-standard particle in the final state can take place (notably $W^+H^-, h\tilde{h}_1^*, h\tilde{h}_2^*, Z\tilde{h}_2^*$); such processes completely dominate and $\alpha \approx 1$.

The value of the SI cross section for the same parameters is displayed in Fig. 1 right panel. The region where $\Omega h^2 \approx 0.1$ just satisfies the Xenon100 bound [196]. Note that to achieve that it was necessary to have an almost pure singlet dark matter. Heavier dark matter satisfy easily the direct detection bounds, although their abundance is too low to explain all of the dark matter.

4 CONCLUSIONS

We have formulated scalar dark matter models with the minimal particle content in which dark matter stability is due to the discrete Z_N symmetry, $N > 2$. Already the minimal models containing one extra scalar singlet and doublet possess non-trivial dark matter phenomenology. In particular, the annihilation processes with new topologies like $\chi\chi \to \chi X$, where χ is the dark matter and X is any standard model particle, change the dark matter freeze-out process and must be taken into account when calculating the dark matter relic abundance. We have performed an example study of semi-annihilations in the Z_3 symmetric scalar dark matter model by implementing the model to micrOMEGAs and studying the impact of semi-annihilations to the relic abundance and on the predictions of dark matter direct detection. We conclude that in this type of models semi-annihilations may significantly affect the phenomenology and must be taken into account in numerical analyses quantitatively exactly.

ACKNOWLEDGEMENTS

Part of this work was performed in the Les Houches 2011 summer institute. K.K. and M.R. were supported by the ESF grants 8090, 8499, 8943, MTT8, MTT59, MTT60, MJD140, by the recurrent financing SF0690030s09 project and by the European Union through the European Regional Development Fund. A.P. was supported by the Russian foundation for Basic Research, grant RFBR-10-02-01443-a. The work of A.P. and G.B. was supported in part by the GDRI-ACPP of CNRS.